Self-Assembly of Carboxyalkylphosphonic Acids on Metal Oxide Powders

Shane Pawsey, Kimberly Yach, and Linda Reven*

Department of Chemistry, McGill University, 801 Sherbrooke Street West, Montreal, Quebec, Canada H3A 2K6

Received December 19, 2001

The structures formed by adsorption of carboxyalkylphosphonic acids on metal oxide powders were characterized by solid-state NMR and FTIR-PAS (Fourier transform infrared photoacoustic spectroscopy). A series of diacids, $HO_2C(CH_2)_nPO_3H_2$ (n = 2, 3, 11, and 15), were deposited on nonporous TiO_2 and ZrO_2 powders and nanocrystalline ZrO_2 with average particle diameters of 21, 30, and 5 nm, respectively. Solid-state ^{31}P NMR, combined with FTIR-PAS, indicates that the phosphonic acid group binds selectively to the surface, producing a monolayer of carboxylic acid terminated chains. The average chain conformation depends on the substrate in addition to the chain length. Ordered samples display thermal order/disorder transitions similar to other self-assembled monolayer systems. The more restricted chain mobility relative to analogous methyl-terminated chains is attributed to hydrogen-bonding among the pendant carboxylic acid groups. These results demonstrate that phosphonic acids are useful for selectively introducing pendant polar functional groups on metal oxide surfaces.

Introduction

Self-assembled monolayers (SAMs) have been studied as a versatile means of surface modification for a wide range of technologies including bioseparations, catalysis, corrosion resistance, microelectronics, and chemical sensors.[1] Organothiol SAMs remain the most popular system despite being limited to the coinage metals. The selective binding of thiols to gold, as well as the absence of a stable gold oxide surface layer, allows for the incorporation of a wide range of functional groups. With the exception of silica, the surface modification of metal oxides with SAMs has not been as well developed. However, long-chain organic acids have been used to form SAMs on Al_2O_3, CuO_2, AgO,[2] Ta_2O_5,[3] mica,[4] Fe_2O_3,[5] TiO_2, and ZrO_2.[6] One obstacle to modifying metal oxide surfaces with monolayers is the possibility of forming looped structures for bipolar surfactants such as $X(CH_2)_nY$ (X = CO_2H, PO_3H_2; Y = OH, NH_2), where the second group may interact with the surface via ionic or hydrogen bonding interactions. If the interaction of the acid group with the particular metal oxide is sufficiently strong, well-packed monolayers with polar terminal groups can form. For example, looping structures were reported for $HO(CH_2)_{15}CO_2H$ adsorbed on Al_2O_3,[2c] but the same surfactant forms densely packed, all-trans chains on ZrO_2 due to the formation of zirconium carboxylate bonds.[6c]

To assess the suitability of phosphonic acid SAMs for introducing polar functionalities on metal oxide surfaces, we chose as a test case a bifunctional surfactant with two groups which may adsorb strongly on metal oxides: $HO_2C(CH_2)_nPO_3H_2$. Since both carboxylic and phosphonic acids form densely packed monolayers on ZrO_2,[6] it is not immediately apparent whether only one group will bind to the surface leaving the other as a free pendant group. In the case of titania, selective binding of the $-PO_3H_2$ group is expected since phosphonic acids form well-ordered SAMs on TiO_2, but carboxylic acids adsorb so weakly that most of the surfactant is removed during the washing steps.[6b]

When considering the possible structures that may result from a particular surfactant/substrate combination, it is useful to examine the bulk state analogues. A wide range of layered metal carboxyalkylphosphonates have been synthesized to investigate their potential use as ion exchangers, proton conductors, catalysts, and host materials.[7] Divalent metals such as Zn and Fe can form structures where the carbonyl group is connected to the metal center.[7e] In the case of tetravalent metals (Zr, Ti) only the phosphonic acid group coordinates with the metal.

(1) (a) Ulman, A. *Chem. Rev.* **1996**, *96*, 1533. (b) Knobler, C. M.; Schwartz, D. K. *Curr. Opin. Colloid Interface Sci.* **1999** *4*, 46.

(2) (a) Allara, D. L.; Nuzzo, R. G. *Langmuir* **1985**, *1*, 45. (b) Allara, D. L.; Nuzzo, R. G. *Langmuir* **1985**, *1*, 52. (c) Laibinis, P. E.; Hickman, J. J.; Wrighton, M. S.; Whitesides, G. M. *Science* **1989**, *245*, 845. (d) Schlotter, N. E.; Porter, M. D.; Bright, T. B.; Allara, D. L. *Chem. Phys. Lett.* **1986**, *132*, 93. (e) Tao, Y. T. *J. Am. Chem. Soc.* **1993**, *115*, 4350. (f) Tao, Y. T.; Lee. M. T.; Chang, S. C. *J. Am. Chem. Soc.* **1993**, *115*, 9547. (g) Smith, E.; Porter, M. D. *J. Phys. Chem.* **1993**, *97*, 8032. (h) Songdag A. H. M.; Raas, M. C. *J. Chem. Phys.* **1989**, *91*, 4926. (i) Songdag, A. H. M.; Touwslager, F. J. *Langmuir* **1994**, *10*, 1028. (j) Touwslager, F. J.; Sondag, A. H. M. *Langmuir* **1994**, *10*, 0, 1028. (k) Tao, Y. T.; Hietpas, G. D.; Allara, D. L. *J. Am. Chem. Soc.* **1996**, *118*, 6724. (l) Tao, Y. T.; Lin, W. L.; Hietpas, G. D.; Allara, D. L. *J. Phys. Chem. B* **1997**, *101*, 9732. (m) Folkers, J. P.; Gorman, C. B.; Laibinis, P. E.; Buchholz, S.; Whitesides, G. M.; Nuzzo, R. G. *Langmuir* **1995**, *11*, 813. (n) Van Alsten, J. G. *Langmuir* **1999**, *15*, 7605.

(3) (a) Brovelli, D.; Hähner, G.; Ruiz, L.; Hofer, R.; Kraus, G.; Waldner, A.; Schlösser, J.; Oroszlan, P.; Ehrat, M.; Spencer, N. D. *Langmuir* **1999**, *15*, 4324. (b) Textor, M.; Ruiz, L.; Hofer, R.; Rossi, A.; Feldman, K.; Hähner, G.; Spencer, N. D. *Langmuir* **2000**, *16*, 3257. (c) Hofer, R.; Textor, M.; Spencer, N. D. *Langmuir* **2001**, *17*, 4014.

(4) (a) Woodward, J. T.; Ulman, A.; Schwartz, D. K. *Langmuir* **1996**, *12*, 3626. (b) Woodward, J. T.; Schwartz, D. K. *J. Am. Chem. Soc.* **1996**, *118*, 7861. (c) Woodward, J. T.; Doudevski, I.; Sikes, H. D.; Schwartz, D. K. *J. Phys. Chem. B* **1997**, *101*, 7535.

(5) (a) Yee, C.; Kataby, G.; Ulman, A.; Prozorov, T.; White, H.; King, A.; Rafailovich, M.; Sokolov, J.; Gedanken, A. *Langmuir* **1999**, *15*, 7111. (b) Shafi, K. V. P. M.; Ulman, A.; Yan, X.; Yang, N.-L.; Estournès, C.; White, H.; Rafailovich, M. *Langmuir* **2001**, *17*, 5093.

(6) (a) Gao, W.; Dickinson, L.; Grozinger, C.; Morin, F. G.; Reven, L. *Langmuir* **1997**, *13*, 115. (b) Gao, W.; Dickinson, Grozinger, C.; Morin, F. G.; Reven, L. *Langmuir* **1996**, *12*, 6429. (c) Pawsey, S.; Yach, K.; Halla, J.; Reven, L. *Langmuir* **2000**, *16*, 3294.

(7) (a) Alberti, G.; Costantino, U.; Vivani, R.; Peraio, A. *Solid State Ionics* **1991**, *46*, 61. (b)Burwell, D. A.; Thompson, M. E. *Chem. Mater.* **1991**, *3*, 14. (c) Burwell, D. A.; Thompson, M. E. *Chem. Mater.* **1991**, *3*, 730. (d) Cao, G.; Rabenberg, L. K.; Nunn, C. M.; Mallouk, T. E. *Chem. Mater.* **1991**, *3*, 149. (e) Drumel, S.; Janvier, P.; Barboux, P.; Bujoli-Doeff, M.; Bujoli, B. *Inorg. Chem.* **1995**, *34*, 148. (f) Bortun, A. I.; Bortun, L.; Clearfield, A,; Jaimez, E.; Villa-Garcia, M. A.; Garcia, J. R.; Rodríguez, J. *J. Mater. Res.* **1997**, *12*, 1122.

10.1021/la015749h CCC: $22.00
Published on Web 05/31/2002

The resulting lamellar $Zr[O_3P(CH_2)_nCO_2H]_2$ structures consist of planes of metal atoms linked together by phosphonate groups with the organic groups lying above and below the inorganic layer. The pendant acid groups form strong interlayer hydrogen bonds, associating as interlayer dimers. Interesting even/odd effects have been observed for the reactivity of $Zr[O_3P(CH_2)_nCO_2H]_2$ toward guest molecules which was attributed to changes in the orientation of the pendant carboxylic acid group with the number of methylene groups.[8] Given these results, it is not unreasonable to expect that carboxyalkylphosphonic acids will form carboxylic acid terminated surfaces on ZrO_2 and TiO_2.

The chain length is an important variable in regards to whether extended versus looping structures will form. We have found that organic acids and alkanethiols form all-trans extended structures on colloidal and powder substrates above a certain minimum chain length.[9] For the deposition of SAMs on nonplanar substrates, the particle size is another important factor due to the possibility of particle−particle interactions. Au−$S(CH_2)_n$-CO_2H nanoparticles are more extensively hydrogen bonded as compared to SAMs of the same surfactant on planar gold.[10] Only the thiol group of $HS(CH_2)_nCO_2H$ will bind to gold, restricting any particle−particle interactions to hydrogen bonding between the pendant acid groups. In the case of the carboxyalkylphosphonic acids, both acid groups can interact with metal oxide surface and particle−particle interactions may also include bridging structures in which a surfactant molecule binds to two particles. The likelihood of such bridging structures increases with increasing chain length and decreasing particle size. To investigate the influence of the chain length and particle size, a series of carboxyalkylphosphonic acids, HO_2C-$(CH_2)_nPO_3H_2$ (n = 2, 3, 11, and 15), were deposited on nonporous TiO_2 and ZrO_2 powders and nanocrystalline ZrO_2 with average particle diameters of 21, 30, and 5 nm, respectively. The surface bonding, chain conformation, and mobility were characterized by ^{31}P and ^{13}C solid-state NMR and Fourier transform infrared photoacoustic spectroscopy (FTIR-PAS).

Experimental Section

Materials. Nonporous zirconia powder (VP zirconium dioxide, Degussa Corp.) was calcinated at 400 °C overnight to remove any residual organics before use. The reported average particle size is 30 nm with a BET surface area of 40 m^2/g. Titania powder (titanium dioxide P25, Degussa Corp.) with a reported average particle size of approximately 21 nm and a specific surface area of 50 m^2/g was used without further modification. The nanocrystalline zirconia (nanoZrO_2) powder (separated equiaxial single crystals, cubic zirconium dioxide, Advanced Powder Technology Pty. Ltd.) with a particle size of 5 nm and a BET surface area of 140 m^2/g was also used without further modification.

Sample Preparation. $HO_2C(CH_2)_2PO_3H_2$ and $HO_2C(CH_2)_3$-PO_3H_2 were obtained from Lancaster Synthesis, Inc., and used without any further purification, while $HO_2C(CH_2)_{11}PO_3H_2$ and $HO_2C(CH_2)_{15}PO_3H_2$ were synthesized. All other reagents were obtained from Aldrich. Starting with either 12-hydroxydodecanoic or 16-hydroxyhexadecanoic acid, the carboxylic acid group was protected through the formation of an ethyl ester by refluxing in absolute ethanol with 0.1 equiv of acetyl chloride. The resulting ester was then brominated by refluxing in a methylene chloride solution with 1.05 equiv of *N*-bromosuccinimide and 1.1 equiv of triphenylphosphine. The brominated species was phosphonated with triethyl phosphate by the Michaelis−Arbazov reaction.[11] The resulting product $[(H_3CH_2CO)_2OP(CH_2)_xCO_2CH_2CH_3]$ was hydrolyzed by refluxing in a concentrated HCl solution for a period of several days. All samples were purified by recrystallization.

Table 1. Samples, Elemental Analysis, and Estimated Coverage

surfactant $HO_2C(CH_2)_nPO_3H_2$	substrate	elemental analysis, % C	% coverage
$n = 2$	nanoZrO_2	7.5	248
$n = 3$	nanoZrO_2	7.3	182
$n = 11$[a]	nanoZrO_2	8.77	80
$n = 15$	nanoZrO_2	14.5	103
$n = 11$	ZrO_2	3.3	90
$n = 15$	ZrO_2	4.6	94
$n = 2$	TiO_2	1.2	82
$n = 3$	TiO_2	1.2	73
$n = 11$	TiO_2	4.1	90
$n = 15$	TiO_2	5.6	94

[a] The $HO_2C(CH_2)_{11}PO_3H_2$/nanoZrO_2 sample was subjected to additional washings with hot methanol.

For preparation of the adsorbed samples, 0.5 g of metal oxide powder was dispersed in 150−200 mL of acetone by sonication. An acetone solution of the surfactant was prepared by dissolving 2.5 times excess of surfactant required to form a monolayer. The well-dispersed powder was added to the surfactant solution, and the mixture was left to reflux with stirring for 2 days followed by an additional 2 days of annealing. The solids were separated by centrifugation and filtering, then washed with heating and filtering an additional five times to remove any weakly bound surfactant, and finally dried under vacuum. Due to the lower solubility of $HO_2C(CH_2)_{11}PO_3H_2$ in acetone as compared to the other carboxyalkylphosphonic acids, some samples underwent additional washing steps with hot methanol.

Solid-State NMR Spectroscopy. Solid-state ^{13}C NMR spectra (67.92 MHz) were acquired on a Chemagnetics CMX-270 spectrometer with a 7 mm (Doty) or 4 mm (Chemagnetics/Varian) double tuned magic angle spinning (MAS) probes with spin rates of 3 and 6 kHz, respectively. A pulse delay of 2−3 s, 4000−8000 scans, and a contact time of 3 ms were typically used to acquire the ^{13}C cross polarization (CP) MAS spectra. For the variable-temperature (VT) experiments the sample temperature was controlled to ±2 °C with a Chemagnetics temperature controller. The 2D wide-line separation experiment (WISE)[12] employs a ^1H pulse followed by a proton evolution period t_1 that consisted of 128 incremented steps of 1 μs. The evolution period precedes the application of a CP pulse followed by carbon detection with decoupling on the proton channel. This combination of pulses will generate a carbon spectrum that is modulated as a function of the evolution period by the free induction decay of the correlated protons. Typically 512 scans were acquired for each evolution period. Short contact times were used in order to minimize the effect of proton spin diffusion, which tends to equalize the proton line widths. Processed data sets contained 1024 points in the ^{13}C (F_2) dimension and 512 data points in the ^1H (F_1) dimension.

FTIR-PAS. Fourier transform infrared photoacoustic spectra (FTIR-PAS) were acquired on a BioRad spectrometer run at a resolution of 8 cm^{-1}. Each FTIR-PAS spectrum consisted of 64 co-added scans for each monolayer-coated metal oxide sample and 32 scans for bulk samples.

Elemental Analysis. Elemental analysis and calculated coverages for the carboxyalkylphosphonic acid/metal oxide samples are given in Table 1. The coverages were calculated by assuming that each molecule occupies 24 $Å^2$, based on the size of the phosphonic acid group.[6] The longer chains $HO_2C(CH_2)_{11}$-PO_3H_2 and $HO_2C(CH_2)_{15}PO_3H_2$, gave coverages close to a monolayer on all three substrates, ranging between 80 and 104%. On the nanoZrO_2, the shorter chains, $HO_2C(CH_2)_2PO_3H_2$ and

(8) (a) Burwell, D. A.; Valentine, K. G.; Thompson, M. E. *J. Magn. Reson.* **1992**, *97*, 498. (b) Burwell, D. A.; Valentine, Timmermans, J. H.; K. G.; Thompson, M. E. *J. Am. Chem. Soc.* **1992**, *114*, 4144.
(9) Badia, A.; Lennox, R. B.; Reven, L. *Acc. Chem. Res.* **2000**, *33*, 475.
(10) Schmitt, H.; Badia, A.; Dickinson, L.; Morin, F. G.; Lennox, R. B.; Reven, L. *Adv. Mater.* **1998**, *10*, 475.
(11) Bhattacharya, A. K.; Thyagarayan, G. *Chem. Rev.* **1981**, *81*, 415.
(12) (a) Zumbulyadis, N. *Phys. Rev. B* **1986**, *33*, 6495. (b) Tekely, P. *Macromolecules* **1993**, *26*, 7363. (c) Claus, J.; Schmidt-Rohr, K.; Adam, A.; Boeffel, C.; Spiess, H. W. *Macromolecules* **1992**, *25*, 5208. (d) Schmidt-Rohr, K.; Clauss, J.; Spiess, H. W. *Macromolecules* **1992**, *25*, 3273.

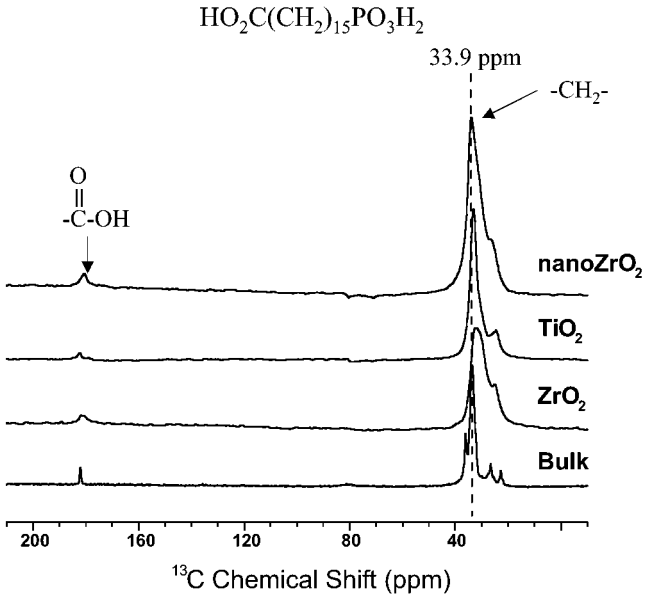

Figure 1. ^{13}C CP MAS NMR spectra of $HO_2C(CH_2)_{15}PO_3H_2$ alone and adsorbed on ZrO_2 (average particle size ~30 nm), TiO_2 (average particle size ~21 nm), and nanoZrO_2 (average particle size ~5 nm). A contact time of 3 ms, a spinning speed of 6 kHz, and 8000 acquisitions were used.

$HO_2C(CH_2)_3PO_3H_2$, had calculated coverages far exceeding a monolayer (182−248%).

Results

^{13}C Solid-State NMR. The ^{13}C CP MAS NMR spectra of $HO_2C(CH_2)_{15}PO_3H_2$ alone and adsorbed on ZrO_2, TiO_2, and the nanoZrO_2 powders are compared in Figure 1. As observed previously for other SAMs, the methylene resonances broaden and shift upon adsorption. The carbonyl signals are also broadened but not as much as for fatty acids adsorbed on ZrO_2 where the resonance is broadened into the baseline.[6c] The inner methylene chemical shifts, $\delta(CH_2)$, show the influence of the substrate on the average chain conformation. Whereas $\delta(CH_2)$ ranges between 29 and 30 ppm in solution due to an equilibrium population of trans/gauche conformations, $\delta(CH_2)$ shifts downfield to 33−34 ppm for crystalline all-trans chains due to the γ-gauche effect.[13] $\delta(CH_2)$ is 33.9 ppm for $HO_2C(CH_2)_{15}PO_3H$ on the nanoZrO_2, indicating all-trans extended chains. On the lower surface area TiO_2 and ZrO_2 powders, the methylene chemical shifts of 33.2 and 32.5 ppm, respectively, reflect a higher population of gauche defects.

The ^{13}C and ^{31}P CP MAS NMR of $HO_2C(CH_2)_nPO_3H_2$, n = 2, 3, 11, and 15, adsorbed on the three different substrates are shown in Figures 2−4. The ^{13}C chemical shifts for the inner methylene carbons for the longer chains (n = 11, 15) are listed in Table 2. Monolayers of $HO_2C(CH_2)_{11}PO_3H_2$ have methylene chemical shifts lower than the n = 15 chain shifts, indicating more gauche defects. The ^{13}C NMR spectra of the two shortest chains, $HO_2C(CH_2)_nPO_3H_2$, n = 2 and 3, are shown only for the nanoZrO_2. On the ZrO_2 and TiO_2 powders, the ^{13}C signal intensities of the n = 2 and 3 chains are very weak due to the relatively low specific surface areas of these substrates. On the nanoZrO_2, the two shortest chains, n = 2 and 3, display relatively strong ^{13}C CP MAS NMR signals despite the low number of methylene carbons. The signal intensity reflects both the high specific surface area of the nanocrystalline zirconia and the fact that the short-chain samples on the nanoZrO_2 contain an excess amount not removed by the multiple washing steps (Table 1).

2D Wide-Line Separation Experiment (WISE) and Variable-Temperature ^{13}C Solid-State NMR. In rigid, crystalline organic solids, the static proton line widths typically range between 50 and 70 kHz but will be reduced by the presence of molecular motion. The proton line widths associated with the inner methylene carbons of $HO_2C(CH_2)_nPO_3H_2$, n = 11 and 15, for the three different substrates were extracted from 2D WISE and are listed in Table 2. The methylene proton line widths of all samples are reduced compared to the crystalline bulk surfactants (55−60 kHz). However, the proton line widths of the n = 15 chains are significantly larger than those of the n =11 chains, showing that the motion is somewhat more restricted.

The thermal stability of the chain order was probed by recording the variable-temperature ^{13}C MAS spectra of the $HO_2C(CH_2)_{15}PO_3H_2$ on nanoZrO_2, which has a single 33.9 ppm methylene carbon peak at room temperature. As the temperature was raised, a shoulder at 31 ppm gradually grew in due to an increasing population of gauche defects. The intensity of the gauchoid peak at 31 ppm surpassed that of the 33.9 ppm transoid peak between 75 and 80 °C. Upon cooling the sample back to room temperature, the ^{13}C spectrum completely returns to its previous state. Since the efficiency of cross-polarization is known to decrease with increasing mobility, the relative intensities were also monitored by direct polarization and were similar to the CP MAS results. $HO_2C(CH_2)_{15}PO_3H_2$ on the TiO_2 and ZrO_2 powders showed similar thermal disordering processes between 60 and 70 °C and between 30 and 40 °C, respectively, reflecting the lower degree of order initially present on these substrates.

^{31}P Solid-State NMR. The ^{31}P CP MAS spectra are displayed in Figures 2−4 and the chemical shifts are listed in Table 3. The ^{31}P NMR spectra of the carboxyalkylphosphonic acids adsorbed on the ZrO_2 and TiO_2 powders are identical to those reported for the alkylphosphonic acids on the same substrates.[6a,b] The phosphonic acid ^{31}P chemical shift changes from 31.5 to 24 ppm upon adsorption on the ZrO_2 powder and the resonance is considerably broadened as compared to the unbound acid. The large line width arises from a distribution of binding sites and modes of the POH headgroup on the heterogeneous ZrO_2 surface.[6a] Phosphonic acids interact more weakly with TiO_2,[14] as indicated by the smaller change in the chemical shift (28 ppm) and smaller degree of line broadening. The ^{31}P NMR spectra of $HO_2C(CH_2)_nPO_3H_2$, n = 2, 3, 11, and 15, on the nanoZrO_2 show more peaks due to the presence of excess surfactant and the formation of a small quantity of bulk metal phosphonate. The broad component present in all of the spectra at 23−24 ppm is assigned to phosphonate groups directly bound to the zirconia surface. The sharp components which are shifted slightly from the broad component centered at 24 ppm are assigned to phosphonic acid groups which are weakly interacting with the surface via hydrogen bonding interactions. In some samples, a small amount of bulk metal phosphonate was produced, as indicated by peaks at 7−8 ppm. These peaks were also observed previously for octadecylphosphonic acid on ZrO_2 and TiO_2 after extended reaction times.[6b]

FTIR Photoacoustic Spectroscopy (FTIR-PAS). The FTIR-PAS spectra for $HO_2C(CH_2)_nPO_3H_2$, n = 2, 3,

(13) Tonelli, E. *NMR Spectroscopy and Polymer Microstructure*; VCH Publishers: New York, 1989.

(14) (a) Gawalt, E. S.; Avaltroni, M. J.; Koch, N.; Schwartz, J. *Langmuir* **2001**, *17*, 5736. (b) Guerrero, G.; Mutin, P. H.; Vioux, A. *Chem. Mater.* **2001**, *13*, 4367.

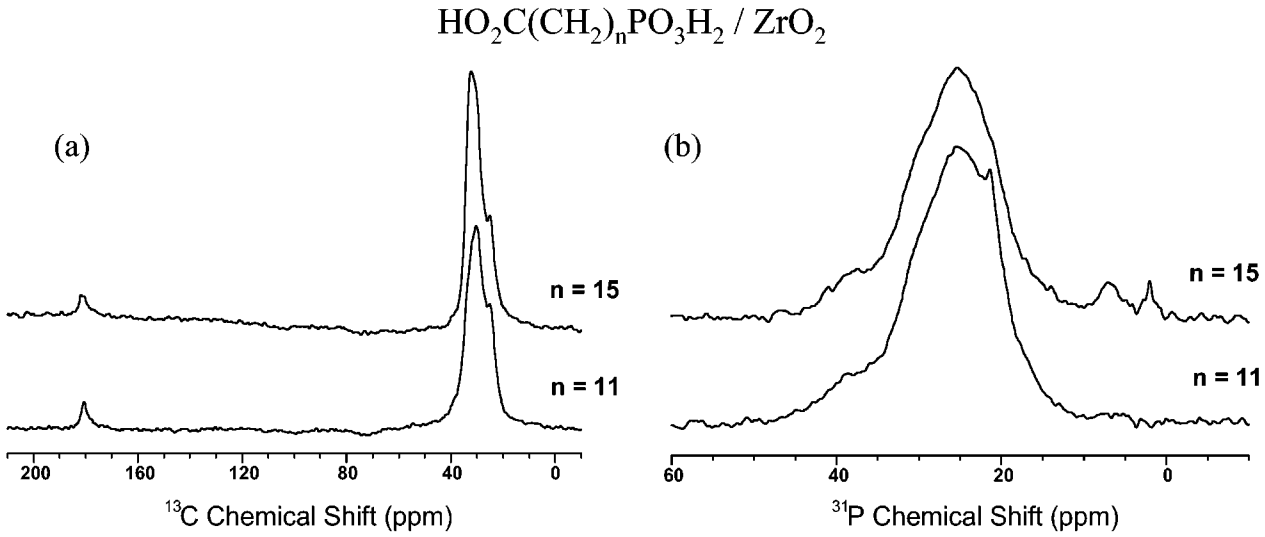

Figure 2. (a) ^{13}C and (b) ^{31}P CP MAS NMR spectra of $HO_2C(CH_2)_nPO_3H_2$, $n = 11$ and 15, adsorbed on ZrO_2 (average particle size ~30 nm).

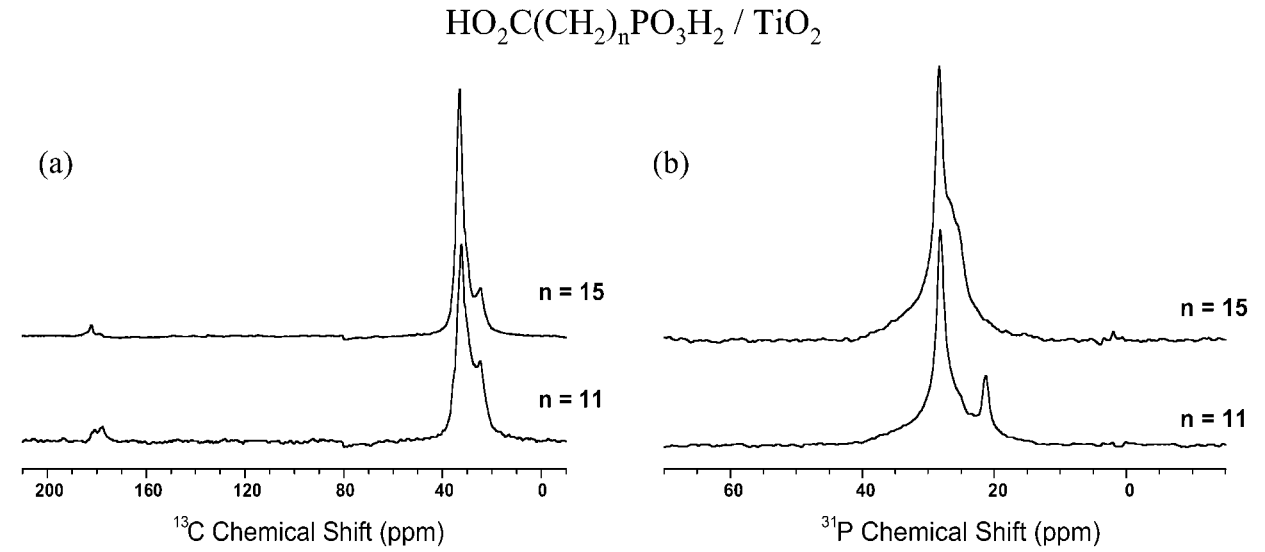

Figure 3. (a) ^{13}C and (b) ^{31}P CP MAS NMR spectra of $HO_2C(CH_2)_nPO_3H_2$, $n = 11$ and 15, adsorbed on TiO_2 (average particle size ~21 nm).

11, and 15, on the three substrates are presented in Figures 5−8 and the frequencies are listed in Table 3. In crystalline alkanes, where the methylene chains are in an all-trans conformation, the asymmetric methylene stretch typically appears at 2917 cm^{-1} as compared to 2925 cm^{-1} in the liquid state. Although the spectral resolution was low (8 cm^{-1}), the asymmetric methylene stretching frequencies from the PAS-FTIR spectra confirm that the $n = 15$ chains are generally more ordered than $n = 11$.

In the carbonyl stretching region, all four samples display strong sharp bands between 1680 and 1710 cm^{-1} that are assigned to the ν(C═O) stretch of a hydrogen bonded carboxylic acid group. The ν(C═O) stretch of carboxylic acid dimers typically lies between 1700 and 1720 cm^{-1} while free non-hydrogen-bonded carboxylic acid groups are generally found between 1735 and 1760 cm^{-1}. The ν(C═O) bands of adsorbed $HO_2C(CH_2)_nPO_3H_2$, $n = 15$ and 11, are at 1711−1716 cm^{-1} as compared to 1705 cm^{-1} for the bulk long-chain acids. In the case of simple fatty acids adsorbed on zirconia, this band is absent since the carboxylic acid groups bind to the surface and are completely converted to zirconium carboxylate groups (ν_{as}(C−O) ~ 1540 cm^{-1}).[6c] In nanoZrO_2 samples (Figure 8) and $HO_2C(CH_2)_2PO_3H_2$ on the ZrO_2 powder (Figure 6), there are broad weak bands that fall in the same region as the carboxylate stretches. These bands may be due to the formation of some zirconium carboxylate. The C−H wag, which is stronger in the long-chain samples, also occur in this region at ~1470 cm^{-1}. Very broad bands in the carboxylate region are also present in the spectra of the untreated ZrO_2 due to adsorbed atmospheric CO_2, which is known to form a variety of carbonate species on zirconia.[15] However these species appear to be displaced by the carboxyalkylphosphonic acids. The relative intensities of the bands in the carboxylate region compared to the C═O stretching band decrease with increasing chain length of the carboxyalkylphosphonic acids. Figure 5 compares the FTIR-PAS spectra of $HO_2C(CH_2)_{15}PO_3H_2$ on all three substrates. The carboxylate bands are much weaker in the spectra of the monolayers on the lower surface area ZrO_2 powder and are absent for the TiO_2 powder. The ZrO_2 samples also show a strong broad band at ~1100−1040 cm^{-1} in the P−O stretching region which is characteristic of the adsorbed phosphonate group.[6b]

(15) Bachiller-Baeza, B.; Rodriguez-Ramos, L.; Guerrero-Ruiz, A. *Langmuir* **1998**, *14*, 3556

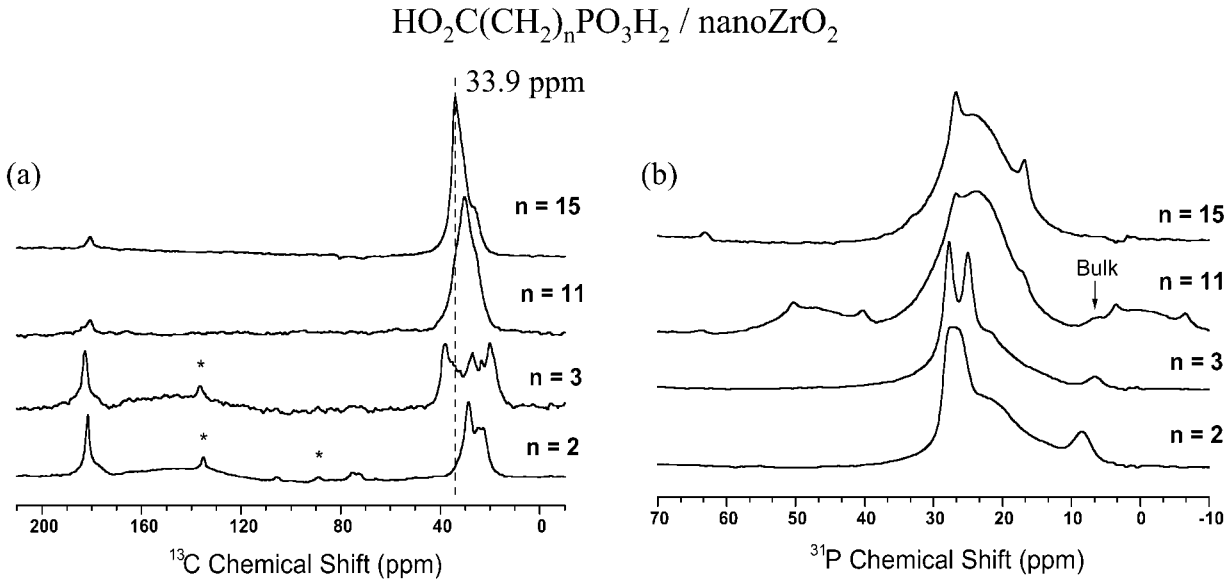

Figure 4. (a) ^{13}C and (b) ^{31}P CP MAS NMR spectra of $HO_2C(CH_2)_nPO_3H_2$, $n = 2$, 3, 11, and 15, adsorbed on nanoZrO2 (average particle size ~5 nm).

Table 2. ^{13}C Chemical Shifts and ^{1}H Line Widths

surfactant $HO_2C(CH_2)_nPO_3H_2$	substrate	methylene ^{13}C chemical shift (ppm)	methylene ^{1}H line widths (kHz)
$n = 11$[a]	nanoZrO2	31.0	28
$n = 15$	nanoZrO2	33.9	47
$n = 11$	ZrO2	31.9	26
$n = 15$	ZrO2	32.5	35
$n = 11$	TiO2	32.3	32
$n = 15$	TiO2	33.2	43

[a] The $HO_2C(CH_2)_{11}PO_3H_2$/nanoZrO2 sample was subjected to additional washings with hot methanol.

Since TiO_2 has a strong adsorption band in this region, the P−O bands cannot be detected.

Competitive Adsorption of RPO_3H_2 and RCO_2H. Two competitive adsorption studies of long- and short-chain alkylphosphonic and carboxylic acids on the two different ZrO_2 substrates were carried out. The acids were chosen so as to have the same number of methylene carbons. Nonadecanoic acid ($CH_3(CH_2)_{18}CO_2H$) and octadecylphosphonic acid ($CH_3(CH_2)_{18}PO_3H_2$) were coadsorbed from acetone on the ZrO_2 powder (ca. 40 m^2/g). Acetone, was chosen as the solvent since it was used to adsorb the carboxyalkylphosphonic acids as well as the fatty acids and alkylphosphonic acids in earlier studies.[6] The following ratios, given in monolayer equivalents (the amount needed to form a complete monolayer), were used for RCO_2H/RPO_3H_2: 2.5:0.5, 3:1, 2:1, 1:1, 1:2, 1:3, and 0.5:2.5. FTIR bands associated with zirconium carboxylate (1540, 1460 cm^{-1}) were observed only for the 2.5:0.5 ratio of carboxylic acid to phosphonic acid, that is, adsorbed carboxylate was only detected when less than a monolayer equivalent of the phosphonic acid is present. Even when 3 monolayer equivalents of the nonadecanoic acid with only 1 monolayer equivalent of the octadecylphosphonic acid were used, no zirconium carboxylate bands were observed, despite the large excess amount of the carboxylic acid.

The competitive adsorption of short-chain carboxylic and phosphonic acid on the nanoZrO2 yielded similar results. Ethylphosphonic acid ($CH_3CH_2PO_3H_2$) and propionic acid ($CH_3CH_2CO_2H$) were coadsorbed on the nanoZrO2 from acetone. The FTIR-PAS spectrum of the untreated nanoZrO2 shows very broad bands at ~1566 and ~1355 cm^{-1} due to carbonate species formed from adsorbed CO_2.[15] These bands vanish when the nanoZrO2 is treated with ethylphosphonic acid, showing that the phosphonic acid completely displaces any adsorbed carbonates. When the nanoZrO2 was treated with mixtures of ethylphosphonic and propionic acids, zirconium carboxylate bands at 1540 and 1460 cm^{-1} were observed only when less than a monolayer equivalent of the ethylphosphonic acid is present.

Discussion

Carboxyalkylphosphonates on the Low Surface Area TiO_2 and ZrO_2 Powders. Long-chain phosphonic and carboxylic acids have both been previously shown to form highly ordered self-assembled monolayers on ZrO_2 powder (average particle size ~ 30 nm) for $n > 16$, where n is the number of methylene carbons.[6] The competitive adsorption studies of the two acids on ZrO_2 powder indicate that phosphonic acids have a much stronger affinity for zirconia as compared to carboxylic acids. However, the different solubilities of the fatty acids versus alkylphosphonic acids are an important factor that cannot be eliminated. The alkylphosphonic acids are generally much less soluble than the fatty acids in most solvents including acetone. Nevertheless, the spectroscopic results point toward attachment of long-chain carboxyalkylphosphonates solely via the phosphonate group on the ZrO_2 powder. For the longest bifunctional chain, $n = 15$, the combination of (i) an all-trans chain conformation, (ii) a monolayer surface coverage, (iii) a strong free acid C=O stretching band, and (iv) the absence of carboxylate bands, rules out the presence of a significant number of looping structures. The ^{31}P NMR spectra show that the binding mode of the phosphonate group is similar to that produced by the adsorption of alkylphosphonic acids on ZrO_2. The intermediate chain length, $HO_2C(CH_2)_{11}PO_3H_2$, has more gauche defects, but the coverage and the strong C=O band at 1716 cm^{-1} are also consistent with preferential attachment via the phosphonate headgroup. In the case of the very short chains, a certain proportion of the carboxylic acid groups also interact with the surface since an IR band at ~1560 cm^{-1} in the carboxylate region is observed for $HO_2C(CH_2)_2PO_3H_2$ on ZrO_2 powder in addition to the C=O band at 1724 cm^{-1} (Figure 6 and Table 3). The presence of residual carbonate contaminants giving rise

Table 3. ^{31}P Chemical Shifts and FTIR-PAS Frequencies

surfactant $HO_2C(CH_2)_nPO_3H_2$	substrate	^{31}P chemical shifts (ppm)	ν_{as}(CH) (cm^{-1})	ν(C=O) (cm^{-1})	ν_{as}(C−O) (cm^{-1})
$n = 2$	nanoZrO_2	27.5(s), ~23 (b), 8.4(s)		1716/1685	1558
$n = 3$	nanoZrO_2	27.7(s), 25 (s), ~23 (b)		1716/1681	1558
$n = 11$	nanoZrO_2	24.5(s), ~23(b)	2924	1712	1550 (w)
$n = 15$	nanoZrO_2	24.7(s), ~24(b),16(s)	2920	1712	1558 (w)
$n = 2$	ZrO_2	~21(b)		1724	1560
$n = 11$	ZrO_2	~25 (b)	2924	1716	
$n = 15$	ZrO_2	~25(b), 7.1(s)	2920	1716	
$n = 2$	TiO_2	27.0		1722	
$n = 3$	TiO_2	27.0		1721	
$n = 11$	TiO_2	28.4	2924	1716	
$n = 15$	TiO_2	28.3	2919	1711	

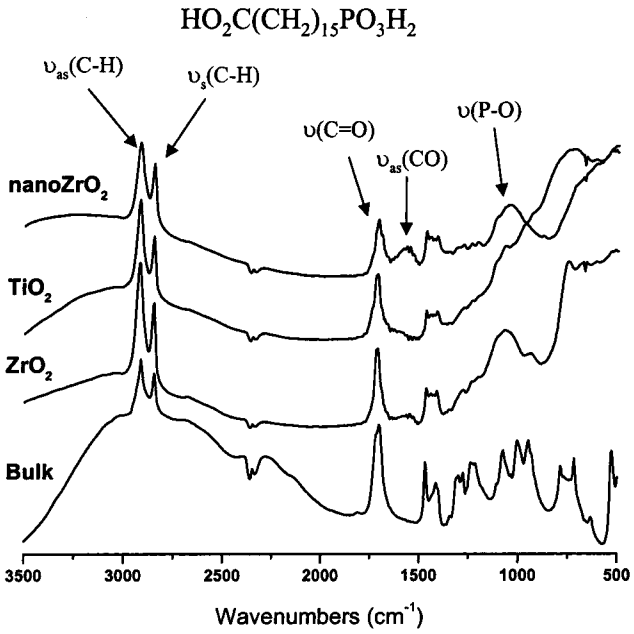

Figure 5. FTIR-PAS spectra of $HO_2C(CH_2)_{15}PO_3H_2$ alone and adsorbed on ZrO_2, TiO_2, and nanoZrO_2.

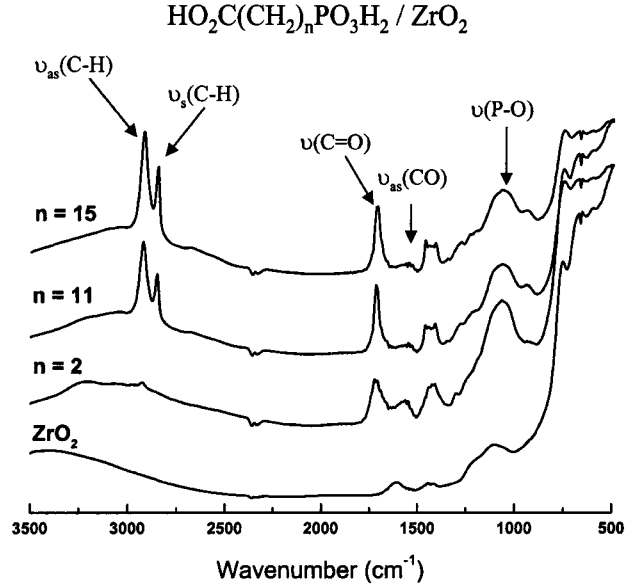

Figure 6. FTIR-PAS spectra of $HO_2C(CH_2)_nPO_3H_2$, $n = 2$, 11, and 15, adsorbed on ZrO_2.

to these carboxylate bands can probably be ruled out since ethylphosphonic acid was found to displace these species.

The same extended chain structures with pendant CO_2H groups form when long-chain carboxyalkylphosphonic acids are adsorbed on TiO_2 although the interaction of the

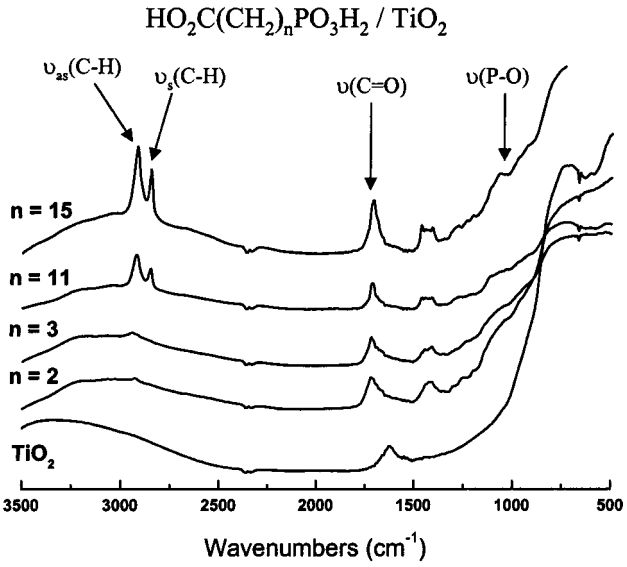

Figure 7. FTIR-PAS spectra of $HO_2C(CH_2)_nPO_3H_2$, $n = 2$, 3, 11, and 15, adsorbed on TiO_2.

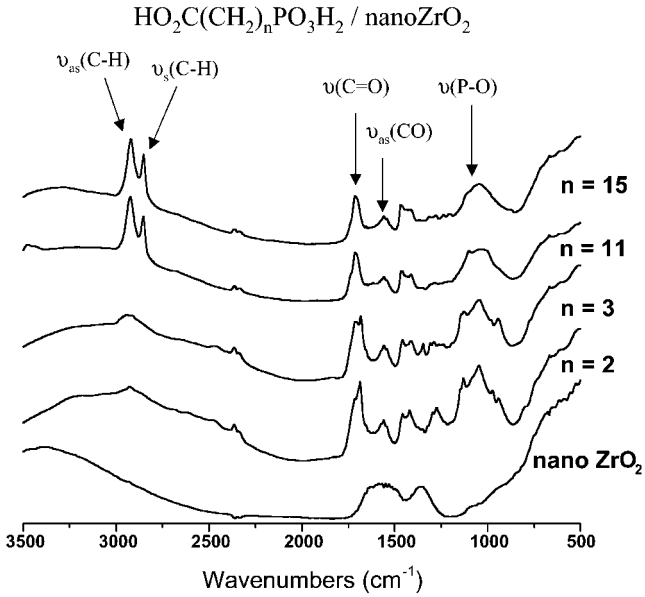

Figure 8. FTIR-PAS spectra of $HO_2C(CH_2)_nPO_3H_2$, $n = 2$, 3, 11, and 15, adsorbed on nanoZrO_2.

phosphonate group with the substrate is somewhat weaker. Unlike the case of ZrO_2, the short-chain molecules ($n = 2$, 3) interact solely via the phosphonate group on TiO_2. Several relevant studies concerning the modification of TiO_2 with phosphonic acids have recently appeared.[14] Gawalt and co-workers reported that the adsorption of alkanephosphonic acids on the native oxide surface of

titanium followed by drying and then heating to 120 °C produced strongly surface-bound films. This self-assembly/heating procedure was applied to $HO_2C(CH_2)_nPO_3H_2$, n = 2 and 3, and the authors also concluded that the attachment occurs solely via the phosphonic acid group.[14a]

Influence of the Particle Size: Carboxyalkylphosphonates on the ZrO_2 Nanopowder. The average particle size was found to be a strong factor in the adsorption behavior of the carboxyalkylphosphonic acids. With decreasing particle size, the effect of the surface curvature and/or particle−particle interactions can become important. Studies of alkanethiol SAMs on gold nanoparticles (average diameter 2−3 nm) show that extensive intercalation of chains between neighboring particles is present.[9] As mentioned earlier, a FTIR and ^{13}C solid-state NMR study of $HO_2C(CH_2)_7SH$ SAMs on gold nanoparticles indicated that the pendant carboxylic acid groups are more extensively hydrogen bonded as compared to SAMs of the same surfactant on a planar gold surface.[10] Furthermore, these carboxylic acid functionalized gold nanoparticles displayed a high degree of conformational order that was thermally stable to over 100 °C despite the relatively short chain length. This behavior was attributed to the possibility of forming both intramonolayer and interparticle hydrogen bonds.[9]

The long-chain carboxyalkylphosphonic acids, n = 11 and 15, form structures on the nanoZrO_2 similar to those on the lower surface area powders. However, the thermal stability of the chain order is much higher on the nanoZrO_2. Chain disordering for $HO_2C(CH_2)_{15}PO_3H_2$ adsorbed on the nanoZrO_2 occurs between 75 and 80 °C as compared to the ZrO_2 powder where the chains disorder between 30 and 40 °C. Proton line width measurements indicate that the chain motion of the carboxyalkylphosphonate SAMs on all three substrates is more restricted as compared to the analogous methyl-terminated SAMs. The methylene proton line widths of the transoid component of octadecylphosphonate SAMs on TiO_2 and ZrO_2 powders range between 20 and 23 kHz,[6b] significantly smaller than the 35−43 kHz line widths measured for $HO_2C(CH_2)_{15}PO_3H_2$ on the same substrates. On the nanopowder, the chain mobility is even more restricted, since a proton line width of 47 kHz was measured for $HO_2C(CH_2)_{15}PO_3H_2$/nanoZrO_2.

The higher degree of conformational order and more restricted mobility are due to more extensive hydrogen bonding of the pendant CO_2H groups and/or higher coverages of the carboxyalkylphosphonic acids on the nanopowder. Alkylphosphonic and carboxylic acids have higher coverages on the nanoZrO_2 (∼90−100%)[16] as compared to the Degussa ZrO_2 powder (∼70−90%).[6b,c] This difference may be partly due to the different morphologies of the two ZrO_2 powders. Whereas the nanopowder consists of separate 5 nm diameter crystallites, the Degussa powders are highly aggregated and not all of the geometrical surface area may be readily accessible to the surfactant.

We found that complete removal of the excess surfactant via the multiple washing steps was more difficult in the case of the carboxyalkylphosphonates on the nanopowders. In addition to the difficulty of washing and centrifuging very small particles, the persistence of excess diacid may be related to the initial formation of carboxylic acid functionalized surfaces via the preferential binding of the phosphonate group. The excess diacid may be strongly hydrogen bonded to the carboxylic acid functionalized particles, making it difficult to remove via the multiple washing steps. Coverages higher than a monolayer were obtained for the very short chain carboxyalkylphosphonic acids on the nanoZrO_2. The ^{31}P NMR spectra of these samples contain large narrow components at 24.5−27.7 ppm, attributed to phosphonate groups attached via hydrogen bonding interactions in addition to the broad components at ∼23−24 ppm, assigned to phosphonate groups directly bound to the metal oxide surface. The deposition solvent, acetone, is not a competitor for hydrogen bonding, but when the short-chain samples on the nanoZrO_2 were also washed with a small amount of water, these narrow ^{31}P components were removed, leaving only the broad component. Both the phosphonic and carboxylic acid groups of the excess diacid can hydrogen bond to the surface-bound pendant carboxylic acid groups. Such a configuration is more likely for the very short chain carboxyalkylphosphonic acids which lack the chain−chain hydrophobic interactions to promote the assembly of extended chains (i.e., standing up versus lying flat on the surface). This picture is supported by recent high-resolution ^1H double quantum and $^1H-^{31}P$ heteronuclear correlation NMR studies which confirm the presence of hydrogen bonding between carboxylic and phosphonic acid groups of the short-chain carboxyalkylphosphonic acids on the nanoZrO_2. [16] The $^1H-^{31}P$ heteronuclear NMR experiments show that only the narrow ^{31}P components are involved in these hydrogen-bonded structures. This hydrogen-bonded structure on the surface differs from the bulk state since no hydrogen bonding between CO_2H and PO_3H_2 groups is detected in the bulk diacids by these experiments, only acid homodimers are present.[16] Further information comes from the FTIR spectra. Bulk $HO_2C(CH_2)_2PO_3H_2$ shows a ν(C=O) band at 1718 cm^{-1}. For this same molecule adsorbed on the nanoZrO_2, there are two ν(C=O) bands at 1716 and 1685 cm^{-1}, assigned to hydrogen-bonded carboxylic acid groups. These two bands may arise because the pendant CO_2H groups of the directly bound layer are hydrogen bonded to the two different types of acid groups (CO_2H and PO_3H_2) of the excess diacid.

A final difference between the two zirconia substrates concerns the relative amount of carboxylate which is detected. Whereas the adsorption of $HO_2C(CH_2)_nPO_3H_2$, n = 15 and 11, on the ZrO_2 powder produced little if any carboxylate, significant carboxylate bands are detected on the nanoZrO_2 for all chain lengths. In addition to differences in the average particle size and the morphology, there may be differences in the distribution and relative strengths of the binding sites for phosphonic and carboxylic acid groups on the two types of zirconia. Whereas the Degussa powder is a poorly crystalline mixture of monoclinic and tetragonal zirconium dioxide, the nanoZrO_2 is highly crystalline, cubic zirconium dioxide. Since the longer chain, n = 15, is in an extended all-trans conformation on the nanoZrO_2, a significant number of looping structures giving rise to surface carboxylate bonds is unlikely. Likewise, the high coverage would seem to preclude a significant population of bridging structures in which a single molecule is attached to two zirconia particles. Unlike the Degussa ZrO_2 powder, the carboxyalkylphosphonates on the nanoZrO_2 all display narrow components in the ^{31}P spectra, although these components are small in the case of the n = 11 and 15 chains. The presence of the narrow ^{31}P components, assigned to weakly interacting phosphonate groups, combined with the carboxylate bands in the FTIR spectra, raises the possibility that some surfactants are attached via the carboxylate group rather than the phosphonate group on the nanoZrO_2.

(16) Pawsey, S.; McCormick, M.; Yach. K.; Reven, L.; Spiess, H. W. Unpublished results.

Summary

The adsorption behavior of carboxyalkylphosphonic acids demonstrates that phosphonic acids can be used to functionalize metal oxide surfaces with pendant polar groups. A longer chain length to promote extended chain structures may be required when the additional polar functionality also has a strong affinity for a particular metal oxide as in the case of carboxylic acids and zirconia. Hydrogen bonding interactions between the terminal carboxylic acid groups leads to more restricted chain mobility and a higher thermal stability of the chain order. In the case of high surface area substrates, the morphology and average particle size as well as the crystallographic phase can be important factors as demonstrated by the presence of some carboxylate surface bonds, higher chain order, and excess carboxyalkylphosphonic acid on the nanocrystalline zirconia.

Acknowledgment. Financial support from the National Science and Engineering Research Council (NSERC) and the Le Fonds FCAR is gratefully acknowledged. The authors thank Professor Thomas Ellis and Craig Hyett of the Université de Montreal for access to the FTIR-PAS spectrometer.

LA015749H